COMMUNICATIONS IN
SCIENCE AND TECHNOLOGY
Homepage: cst.kipmi.or.id

Ionic liquid ultrasound-assisted extraction (IL-UAE) for duck feather keratin and in silico evaluation as a potential procollagen n-endopeptidase inhibitor

Maria Monica Sianita Basukiwardojo[a,*], Nita Kusumawati[a], Mahanani Tri Asri[b], Shod Abdurrachman Dzulkarnain[c], Achmad Naufal Al Hafidl[a], Ashabul Kahfi[a], Mutiara Azfa Nabila[a], Ferdiansyah Setiawan[a], Luthfiyah Isyrak[a], Khofifatul Rahmawati[a]

[a]*Department of Chemistry, Universitas Negeri Surabaya, Surabaya 60231, Indonesia*
[b]*Department of Biology, Universitas Negeri Surabaya, Surabaya 60231, Indonesia*
[c]*Department of Medical Science, Universitas Negeri Surabaya, Surabaya 60231, Indonesia*

Article history:
Received: 28 February 2025 / Received in revised form: 23 May 2025 / Accepted: 24 May 2025

Abstract

This research aims to optimize keratin extraction from duck feathers using an eco-friendly ionic liquid-ultrasound-assisted extraction (IL-UAE) method and evaluate its potential applications in tissue engineering. It investigated the effects of deposition pH (1-6), ultrasonication temperature (40-60°C), and time (60-180 min) on extraction yield and physicochemical properties. The results demonstrated the optimal extraction conditions at pH 3, 40°C, and 60 minutes, yielding 82% keratin with a 0.50 mg/mL concentration, while the lowest yield production was found at pH 6 (33%, 0.20 mg/mL). Meanwhile, characterization via FTIR confirmed predominant β-sheet structures with characteristic peaks at 3250-3300 cm^{-1} (N-H/O-H stretching) and 1700-1500 cm^{-1} (C=O stretching). SDS-PAGE revealed pure keratin bands (10-15 kDa), while SEM showed layered, porous morphology suitable for biomaterial applications. Thermogravimetric analysis, furthermore, identified three degradation stages occurred at 0-200°C (3.05% loss), 200-400°C (39.37% loss), and 400-700°C (31.13% loss). Amino acid profiling revealed high L-cystine content (153,064.90-156,926.33 mg/kg) with the significant amounts of glycine (63,958.25-64,064.73 mg/kg), L-proline (77,631.16-77,717.42 mg/kg), and L-leucine (59,111.43-59,198.60 mg/kg). In silico molecular docking studies identified leucine as a promising procollagen N-endopeptidase inhibitor (binding energy -5.0 kcal/mol), which controlled the collagen-breaking and forming process. This ability makes keratin potential to be developed as a scaffold for bone tissue regeneration in medical industry.

Keywords: Keratin; duck feathers; ionic liquid; ultrasound-assisted extraction; procollagen n-endopeptidase inhibitor

1. Introduction

Bone deterioration is a complex problem that affects millions of people worldwide. It is mostly determined by external factors, including tumor resection, trauma, surgical interventions, and degenerative diseases such as osteoporosis and arthritis [1,2]. The prevalence of bone deterioration has increased significantly since 1990 with a projected 2.6-fold increase by 2025 [3,4]. It has then made bone the second most transplanted tissue worldwide with 2 million cases yearly. Major risk factors include age, modern lifestyle, and the complexity of chronic health conditions [2,3,4]. Bone regeneration approaches have undergone rapid development since the last decade. Autogenous and allogeneic bone transplantation has long been the standard method of bone reconstruction; however, the lack of donor availability, high risk of inflammation, and potential for immune system rejection limit the effectiveness of both approaches [2,4].

To address these complexities, the development of regenerative biomaterials has become a significant focus of regenerative medicine research with a number of main goals to create donor-independent solutions, use natural materials to minimize immunological risks, and have optimal integration capabilities with stem cells through superior therapeutic properties. A promising innovative approach is the

* Corresponding author.
Email: mariamonica@unesa.ac.id
https://doi.org/10.21924/cst.10.1.2025.1669

development of porous 3D nanofiber scaffolds, which combine non-toxic synthetic polymers with specific biomaterials [5,6]. Tissue engineering methods are designed to create 3D matrices essential for bone cell proliferation, migration, and differentiation [6,7]. The key characteristics of developable scaffolds include complex 3D architectures with porosity that facilitates nutrient exchange and cell migration and biomaterial compositions that are compatible with biological systems [8,9]. Combining non-toxic synthetic biopolymers with natural biomaterials aims to create a microarchitectural environment that can support optimal bone regeneration [10,11].

Keratin is a natural polymer with several advantages, including biocompatibility, biodegradability, natural abundance, antimicrobial activity, and cellular compatibility that enhances integration with bone [8,12,13]. It is a fibrous protein with 7-20% cysteine amino acid residues, whose oxidation leads to inter- and intramolecular covalent bonds, the source of keratin fiber toughness [14]. Keratin contains the cell adhesion sequences RGD (Arg-Gly-Asp) and LVD (Leu-Asp-Val), also found in extracellular matrix proteins such as fibronectin [15,16].

Of particular interest is the interaction between keratin-derived amino acids and procollagen N-endopeptidase, an enzyme that plays a crucial role in bone metabolism and extracellular matrix remodeling. Procollagen N-endopeptidase is responsible for cleaving the N-terminal propeptide of type I, II, and III procollagens, a critical step in collagen maturation. The inhibition of this enzyme has significant therapeutic implications for bone regeneration as it is able to modulate collagen processing and deposition rates. This modulation is particularly relevant in the context of protein kinase D (PKD) signaling pathways, regulating numerous cellular processes, including cell proliferation and extracellular matrix organization. By targeting the interaction between keratin-derived amino acids and procollagen N-endopeptidase, it might be possible to develop novel therapeutic approaches that enhance bone repair through controlled collagen metabolism and improved scaffold integration.

Containing more than 70%, duck feathers becomes one of the potential alternative keratin sources. Although the keratin content in duck feathers is found lower than chicken feathers (91%), the higher α-keratin content of duck feathers has made their keratin dominated by a spiral-shaped α-helical structure with high stability [17]. This structure can produce more potent and more flexible properties in 3D scaffolds.

Traditional methods for extracting keratin from feathers mostly use strong acids and bases or high-concentration salt solutions [18,19,20]. This multi-stage process can trigger protein degradation. The consumption of large quantities of reagents and improper management will pose a risk of environmental pollution. Although superheated water is a more eco-friendly processing method, it still can break the peptide bonds in protein molecules, consequently leading to protein degradation [21,22]. Developing a new, simpler, and more eco-friendly method for keratin extraction, therefore, is deemed essential.

Ionic liquids (IL), a group of salts that are in the liquid state at relatively low temperatures, are becoming an alternative solvent that is not only eco-friendly and safe but also superior in view of its non-volatile, non-flammable, high chemical and thermal stability and easy recycling [23,24]. They have more excellent solubility compared to traditional solvents [25]. These various advantages have made IL applied in the pre-treatment and catalytic hydrolysis of small molecules and natural macromolecules, including lignocellulosic biomass [26], glycosides [27,28], carbohydrates [29,30,31], and proteins [24,32]. The results showed no significant changes in the degree of polymerization and dispersibility or in obtaining ideal hydrolysis efficiency. Containing various functional anions and cations, IL exhibits strong interactions at hydrogen and peptide bonds in a 3D network structure of associated macromolecules, resulting in efficient dissolution and decomposition [33]. However, long processing times and high costs become the weaknesses of conventional keratin extraction using IL. By means of this method, Polesca et al. (2023) reported 95% keratin recovery after a 5-hour extraction [34]. Therefore, finding an extraction method compatible with IL to reduce chemicals and processing time purposely to result in high extraction efficiency and low costs is something urgent.

Ultrasound-assisted extraction (UAE) has been widely applied in various fields, such as food, biomedicine, and cosmetics. On the one hand, the mechanical vibration effect can increase a contact between material and medium, thereby facilitating a reaction process. On the other hand, acoustic cavitation in the sonication medium can lead to destruction. Mechanical vibration acoustic cavitation can trigger mass transfer and ultimately produce productivity in industry. Cordova et al. (2025) reported the UAE's ability to make optimum anthocyanin yield in a 5-minute winemaking by-product processing [35]. In line with this, Kong et al. (2025) reported the optimum yield of prenylated flavonoids in Sophora flavescens (PFS) (5.97 mg/g) from 28 min UAE using a liquid-to-material ratio of 26 mL/g [36]. Both showed the UAE's success in reducing chemical usage and time processing. However, the use of this method in combination with IL to obtain higher efficiency and eco-friendly properties of keratin extraction, specifically from duck feathers, so far, has never been reported.

This study aims to evaluate the effectiveness and efficiency of UAE using IL and characterize the physical (morphology and crystallinity), chemical (functional groups, hydrogen bonds, and pH parameter analysis), mechanical (tensile strength and elongation), and thermal (TGA curves) properties of the resulting duck feather keratin. Furthermore, this study evaluated the potential of keratin as an optimal PHB/keratin scaffold for bone tissue reconstruction applications through in silico molecular docking analysis. The computational approach investigated an interaction between key amino acids found in duck feather keratin and procollagen N-endopeptidase, an enzyme critical in collagen metabolism and extracellular matrix remodeling. This dual experimental-computational investigation provides comprehensive insights into both the extraction optimization and potential biomedical applications of duck feather keratin, particularly in relation to bone tissue engineering. The in silico study specifically examined how amino acids from keratin might function as the inhibitors of procollagen N-endopeptidase, potentially regulating collagen turnover in bone regeneration applications.

2. Materials and Methods

2.1. Materials

Feathers form freshly slaughtered adult duck were obtained

from duck feather exporters in Bangkalan, Indonesia. Several chemicals required for feather preparation included ethanol (≥96%, Merck, Singapore) for immersing and cleaning, and for extraction it included Sodium Sulfide (Na_2S) (anhydrous, Merck, Singapore) obtained from Cahaya Kimia Indonesia, Sodium Hydroxide (NaOH) (96%; Merck, Singapore), Hydrochloric Acid (HCl) (≥37%; Fluka, Austria), and distilled water.

2.2. Method

2.2.1. Duck feather preparation

Using ethanol extraction purification, duck feathers were cleaned from stains, oil, dirt, and pathogens [37]. 100 grams of duck feather samples were soaked into 1 L of ethanol for 24 hours and dried in an incubator at 34±1°C for 72 hours. The samples were further conditioned in an oven at 60 ± 2°C and 20% RH for 72 hours prior to be ground into powder, as shown in Fig. 1.

Fig. 1. Pre-treatment process to remove all types of contaminants, both organic and inorganic compounds

2.2.2. Ionic liquid solvent preparation

Chemical compounds consisting entirely of cations and anions were in the liquid phase at room temperature (below 100°C). In this case, sodium sulfide (Na_2S), an ionic compound, was dissolved in water to produce ionic liquid, as shown in Fig. 2.

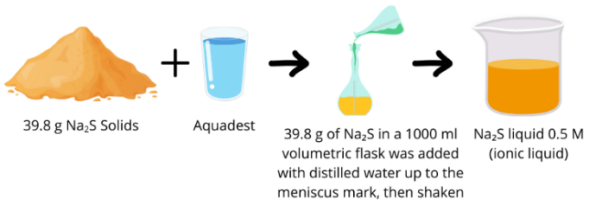

Fig. 2. Pre-treatment process for the preparation of ionic liquid solvent

2.2.3. Extraction of keratin

After grinding, a total of 20 g of duck feather powder was immersed into a Na_2S 0.5 M (ionic liquid) with a ratio of 1:20. The pH of the solution was conditioned at 10.5 using NaOH 0.05 M by referring to Pourjavaheri et al. (2019) [37]. The solution was then heated at a constant temperature of 40°C while continuously stirring by means of an ultrasonicator (Elmasonic S 80 H). Subsequently, 11,648 g of sample was centrifuged using a Centrifuge (Hettich EBA 20) at 10°C for 20 minutes. The supernatant was collected, and the residue was discarded. 7 M HCl was added to obtain a pH of 1-6. The solution was left for 2 hours without heating or stirring. Filtration was then carried out to separate the filtrate and the precipitate obtained. The precipitate was rinsed using distilled water prior to be dried in an oven (Memmert UN55) at 60°C for 48 hours, as shown in Fig. 3 [38,39].

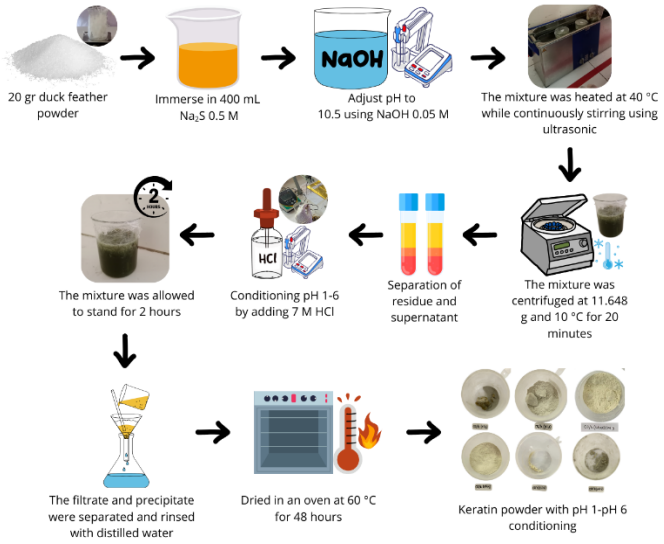

Fig. 3. Schematic of the keratin extraction process steps using the ionic liquid ultrasonic assisted extraction (IL-UAE) method

2.2.4. Yield

Yield and weight loss were determined by following Equation (1)-(3).

$$\%yield = \frac{W_{fk}}{W_{ik}} \times 100 \quad (1)$$

$$\%loss = \frac{W_{ik} - W_{fk}}{W_{ik}} \times 100 \quad (2)$$

$$\%total\ weight\ loss = \frac{W_i - W_{fk}}{W_i} \times 100 \quad (3)$$

where W_{ik} and W_{fk} refer to the weight of wet and dry keratin, respectively, while W_i is the weight of duck feathers.

2.2.5. Concentration of keratin

Keratin concentration was determined using UV-Vis spectrophotometry (Eppendorf AG, Hamburg, Germany) at 280 nm [19].

2.2.6. Fourier transform infrared (FTIR)

The functional groups of keratin powder from various pH conditions were analyzed using an FTIR spectrophotometer (Perkin Elmer Spectrum Two). Spectral data were collected in transmission mode at 4000-650 cm^{-1}, using scanning at a resolution of 4 cm^{-1}.

2.2.7. Scanning electron microscopy (SEM)

To obtain the particle surface morphology, size, and

distribution of duck feather keratin particles, analysis was carried out using Scanning Electron Microscopy (JSM-6510) at the magnifications of 2000x, 10,000x, and 20,000x.

2.2.8. Thermogravimetric analysis (TGA)

To determine the thermal degradation pattern based on keratin mass loss as a function of temperature, analysis was carried out using a Thermogravimetric Analyzer (PerkinElmer TGA Pyris 1) at 30-750°C under nitrogen purge (20 mL/min) and 750-850°C under oxygen purge (20 mL/min) with a heating rate of 20 $Kmin^{-1}$.

2.2.9. Amino acid profiling

The analysis of the type composition and proportion of amino acids making up the keratin protein was carried out through High-Performance Liquid Chromatography (HPLC). It was conducted at room temperature using a LiChrospher 100 RP-18 column (5 mm) with an eluent flow rate of 1.5 mL/minute. Meanwhile, detection was conducted using a Thermo Ultimate 3000 RS Fluorescence Detector with an excitation wavelength of 300 nm and an emission wavelength of 500 nm [19]. The amino acid composition determined the mechanical and biological properties of the duck feather keratin.

2.2.10. Sodium dodecyl sulfate polyacrylamide gel electrophoresis (SDS-Page Gel)

An analysis was carried out to separate protein subunits based on molecular weight using SDS-Page Gel on a polyacrylamide matrix powered by an electric field. The flowing electric charge enables the protein to move through the gel from the negative to the positive pole. Polyacrylamide gel separates molecules based on molecular size and shape. Here, small molecules move faster than large ones.

2.2.11. Liquid chromatography-mass spectrometry (LC-MS)

1 microgram of keratin was incubated with 200 µg/µL sequencing grade trypsin at 37°C overnight. Assimilation was stopped by formic acid (FA) to a final concentration of 1% and drying in a vacuum. The processed keratin was analyzed by fluid chromatography/mass spectroscopy (LC-MS/MS) using a Q-Exactive mass spectrometer (Thermo Logical).

2.2.12. Nuclear magnetic resonance (NMR)

NMR samples were obtained from duck feathers ground into powder using a Rocklabs Ringmill Grinder (with zirconia mill head) for 3 minutes. To obtain NMR spectra of duck feathers, the Agilent DD2 500 MHz NMR spectrometer was equipped with a 4 mm MAS solid-state triple resonance probe, operated at a rotation speed of 10 kHz, scanning 4 (proton) or 4000 (carbon), and a delay time of 5 seconds.

2.2.13. Molecular Docking

The molecular docking analysis used Procollagen N-Endopeptidase Inhibitor protein from RCS Protein Data Bank (PDB ID: 3F1S). Hydrogen atoms and Kollman charges were calculated and added after the cofactors to prepare proteins. Water molecules and metal ions were removed so as not to interfere with the process. Preliminary tests using the CB-Dock application were carried out to obtain information on grid arrangement, cavity size, and vein score, required to make the docking procedure more accurate. Some ligands including amino acids cysteine, leucine, serine, and proline, taken from the Pubchem website, were used. The resulting data then displayed 2D and 3D bond visuals and bonding energy data.

3. Results and Discussion

3.1. Yield

The yield of duck feather keratin was obtained highest at pH 3 (82%) and lowest at pH 6 (33%). Table 1 depicts the details of the yields obtained at various pH values.

Table 1. Yield% keratin duck feather

Sample	Yield%
pH 1	76
pH 2	80
pH 3	82
pH 4	79
pH 5	40
pH 6	33

Keratin tended to aggregate due to the formation of hydrogen bonds and hydrophobic interactions at pH 3 as the ideal pH to form keratin coacervate. The protonation of carboxylic groups (COO-) peaked at pH 3, decreasing electrostatic repulsion and strengthening keratin molecule association. This condition then resulted in consistent and stable development of keratin coacervates. The opposite condition results when excessive protonation triggered a more pronounced phase separation at pH 1-2. On the other hand, the deprotonation of carboxylic groups increases electrostatic repulsion at pH values higher than 3, and reduces the effectiveness of coacervate production [40].

If compared to previous research, the extraction method using Na_2S ionic liquid with pH optimization showed more efficient results. Wang & Tong (2022) developed a keratin extraction method from duck feathers using the imidazol [Bmim]Cl ionic liquid with a yield of 75.1% [52]. As shown by Senthilkumar et al. (2022), keratin was extracted from duck feather using steam flash explosion (at 1.6 MPa for 1min) followed by alkali extraction using 0.4% NaOH for 1 hour with a yield of 42.78% [53]. Although ionic liquid method is claimed to be environmentally friendly, our research results with pH optimization indicated an increase in yield about 7% at pH 3 conditions. This suggests that pH adjustment is not only a simpler approach but also more effective in the keratin extraction process from duck feathers.

3.2. Concentration

Table 2 presents a summary of the concentrations of

extracted keratin at different pH values. Based on the UV-Vis absorbance results, the keratin solution concentration at various pHs correlated with the extraction yield was obtained. This is in line with what was reported by Mengistu et al. (2024) [41]. The higher the keratin yield produced, the higher the concentration of keratin solution dissolved in the medium, as shown by the increased absorbance value at a wavelength of 280 nm.

At pH 3, the highest yield was 82%, aligning with the relatively high concentration of the keratin solution. This was caused by pH conditions that supported keratin aggregation through hydrophobic interactions and hydrogen bonds so that more protein could be dissolved and detected in the solution. On the other hand, at pH 6, the lowest yield of 33% caused a lower solution concentration, indicated by a more negligible absorbance. This was likely due to electrostatic repulsion between keratin molecules, inhibiting solubility and increasing the tendency to precipitation.

This difference in concentration can also be attributed to the stability and structure of keratin at various pHs. At more acidic pH (pH 2–4), the protonation of carboxylic groups (-COO^-) weakened electrostatic repulsion, allowing more keratin to dissolve. Conversely, at higher pH (pH 5–6), deprotonation could increase intermolecular repulsion, reduce solubility, and decrease yield.

Table 2. Extracted keratin concentrations by IL-UAE as estimated using protein absorbance at 280 nm

Sample ID	Conc (mg/mL)	WL400,0 (Abs)
pH 1	0.30	0.117
pH 2	0.45	0.286
pH 3	0.50	0.379
pH 4	0.40	0.256
pH 5	0.25	0.082
pH 6	0.20	0.069

Thus, the relationship between yield and solution concentration shows that extraction pH is critical in determining keratin solubility. This is in line with what Perez-Vila et al. (2024) reported when examining the effect of extraction methods on the composition and solubility of Perennial ryegrass leaf protein concentrate [42]. pH optimization is necessary to obtain high yields and keratin solutions with sufficient concentration for further applications in tissue engineering.

3.3. FTIR

Keratin yield at various pHs showed consistency with the peak reported by Oussadi et al. (2025) [43]. Observing the absorbed amino groups and water, it was detected that the amino groups remained stable in keratin at various pHs. The peak at 3250–3300 cm^{-1} indicates the stretching vibration of the -N-H and -O-H groups of the hydroxyl and amine groups, which are the characteristic of keratin. The decrease in peak intensity at lower pH indicates a decrease in hydrogen bonding capacity under acidic conditions [44].

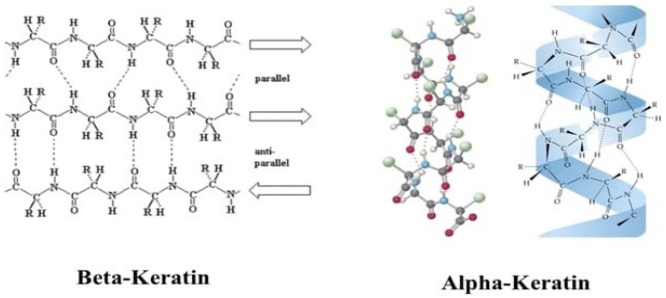

Fig. 4. Structure of (a) α-keratin showing predominant α-helix conformations with coiled-coil structure, and (b) β-keratin displaying characteristic β-sheet arrangement with extended polypeptide chains

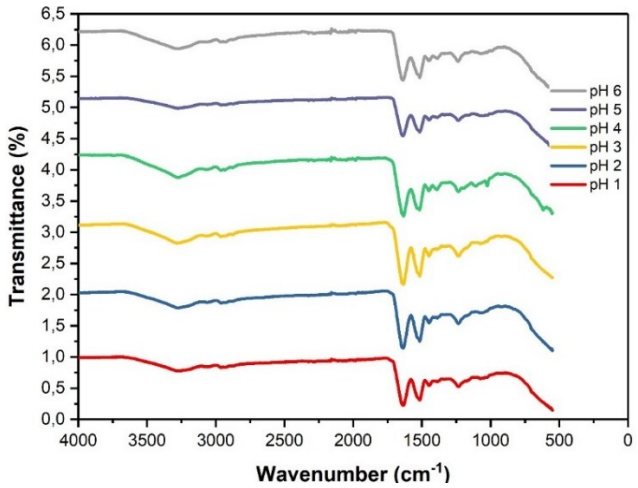

Fig. 5. FTIR spectra of the keratin extracted at different pH conditions (pH 1 - pH 6) showing characteristic absorption bands of functional groups

In the 1700-1500 cm^{-1} region, the appearance of a sharper peak is most likely produced by carbonyl (C=O) stretching vibrations indicating the presence of carboxylic acid or ketone groups, with a slight shift and decrease in intensity at various pH, reflecting the modification of the chemical environment around these groups due to changes in pH. The characteristic amide I bands were observed at 1640–1660 cm^{-1} indicating α-helix structure, and at 1660–1685 cm^{-1} corresponding to β-sheet structure. Meanwhile, the peak at 1200-1000 cm^{-1} can be attributed to the stretching vibration of the C-O or C-N groups, which also experience a specific shift in position and change in intensity at a certain pH [45]. This spectrum analysis provides detailed information regarding changes in molecular interactions and functional group stability of keratin samples in response to environmental acidity (Fig. 5).

Overall, the FTIR results showed that although slight shifts and changes in peak intensity were detected at different pH conditions, several peaks characteristic of the amino, carbonyl, and peptide groups typical of keratin could still be found. Thus, even with the decrease in hydrogen bonding capacity and changes in molecular interactions with changes in pH, keratin still exhibits important bioactivity. The dominant presence of the O-H, C=O, N-H, C-H, and C-N functional groups shows the presence of β-sheet keratin in duck feathers, as shown in Fig. 4.

3.4. SDS-Page gel

SDS-PAGE gel electrophoresis analysis was conducted to determine the atomic mass of the severed protein homologs, pattern, and purity of keratin extracted using Na_2S (Fig. 6). The molecular mass of keratin was calculated using standard markers. SDS-PAGE information revealed that the keratin in this study had the groups of prominent bands and spread ca. 20 kg/mol, representing the atomic mass of concentrated keratin.

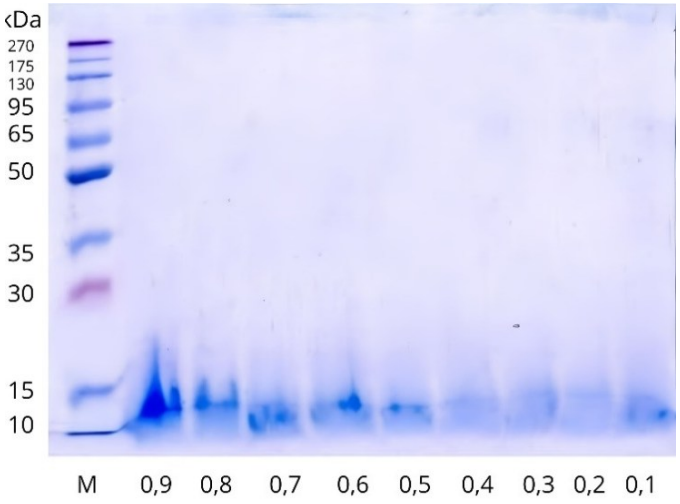

Fig. 6. SDS-PAGE gel electrophoresis of keratin samples showing protein bands at different concentrations, confirming the purity and molecular mass of extracted keratin

SDS-PAGE analysis showed a significant relationship between keratin concentration and band intensity. The strongest bands appeared in samples with higher concentrations (0.9), while their intensity gradually decreased as the concentration decreased to 0.1. The appearance of all bands was consistently at 10-15 kDa (pure keratin in the range of 10-25 kDa), indicating that the same keratin protein was present in all samples. The presence of a single band (without any additional bands) indicates the success of the Na_2S extraction method in producing pure keratin protein [46]. Even at the lowest concentration (0.1), the protein could still be detected, indicating that the extraction method and detection technique were effective and reliable for the analysis of keratin samples.

3.5. SEM

Fig. 7. illustrates the SEM images of keratin. SEM results visualized the keratin surface as a occasionally flat and rough structure formed by several layers of keratin that overlapped each other, similar to the structure of scales. Aggregate was attached to this flat structure. At 20,000x magnification, the aggregate showed a dense porous structure with high porosity. This morphology is found similar to Alvarez's (2024) [47].

It is fundamental to biomaterial applications, such as tissue restoration and wound healing. The observed dispersion of micrometer-sized molecules underlies keratin-based scaffolds' mechanical properties and protein composition. These surface characteristics contribute to increased cellular grip, supplement dispersion, and general biocompatibility, making them suitable for biomedical applications [47].

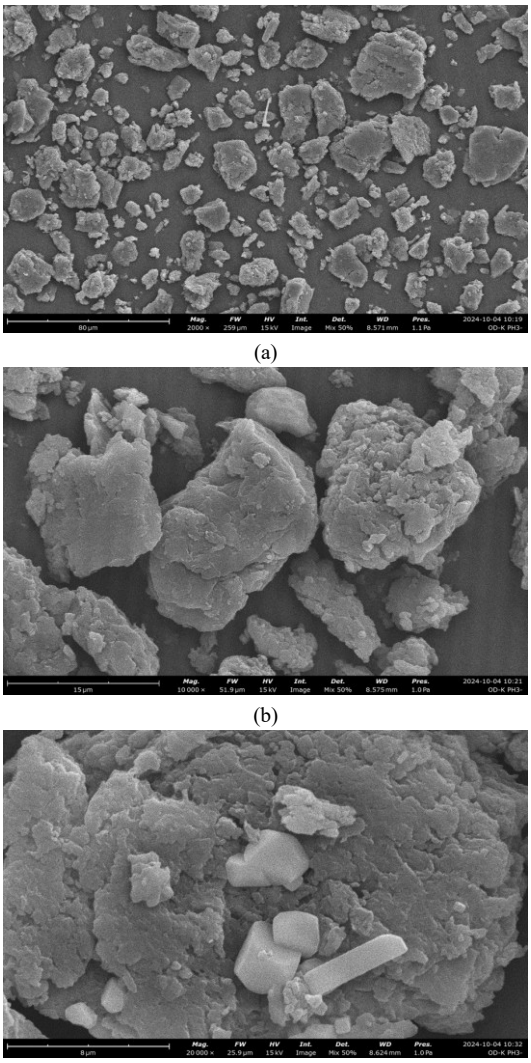

(a)

(b)

(c)

Fig. 7. SEM micrographs of extracted keratin showing: (a) Scale-like overlapping keratin layers with rough surface at 2,000x magnification; (b) Intermediate view revealing aggregated structures between layers at 10,000x magnification; (c) High-resolution image at 20,000x magnification displaying dense porous microstructure with interconnected pores suitable for cellular attachment

3.6. TGA

In Fig. 8, the thermogravimetric analysis (TGA) of duck feather keratin showed three stages of significant thermal degradation. In the first stage (0-200°C), a mass reduction of 3.05068% was detected, which resulted from the dehydration of the keratin sample. A more significant mass reduction was detected in the second stage (200-400°C), i.e. 39.3661%. The degradation of the main structure of keratin, where keratin protein decomposition occurs, including breaking peptide bonds and degradation of amino acid side chains, is a trigger for mass reduction in this second stage. The sharp slope of the curve at this stage indicated a fast degradation rate.

In the third stage (400-700°C), a stage of further degradation of organic residues, mass reduction was slightly lower than that of in the second stage, i.e. 31.1334%. At this high temperature, the carbonization process of the remaining organic material occurred with a curve showing a slightly

gentler decline compared to the second stage. A total mass reduction of up to 73.5% was recorded at 700°C. These results indicated that duck feather keratin has moderate thermal stability with approximately 26.5% of the remaining material likely in ash and fixed carbon. The results of this analysis align with the general characteristics of keratin protein, which undergoes gradual degradation with increasing temperature and the main stage of degradation occurred at 200-400°C [48].

3.7. Amino Acid Profiling

Table 3 presents the complete amino acid profile of duck feather keratin. The analysis of amino acid content revealed the presence of 18 types of amino acids with various concentrations in the keratin samples tested. The highest concentration was observed in L-Cystine, 153,064.90 - 156,926.33 mg/kg. These results indicated L-Cystine as an essential component in the protein structure of duck feather keratin, which plays an important role in forming disulfide bonds stabilizing the protein structure [49]. In contrast, the lowest concentration was observed for L-Methionine, 101.95 - 103.29 mg/kg. Even though its concentration was found low, L-Methionine still has an important role in synthesizing sulfur-containing compounds such as S-adenosylmethionine.

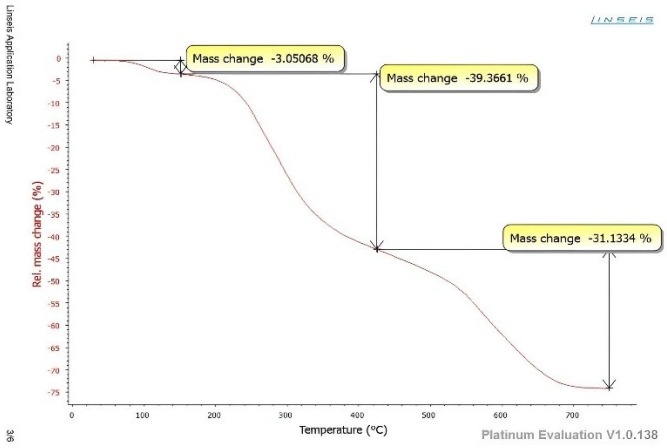

Fig. 8. Thermogravimetric analysis (TGA) curve of duck feather keratin showing three-stage thermal degradation process with corresponding weight loss percentages

Table 3. Amino Acid Profile of Keratin Duck Feather

No	*Parameter*	*Unit*	*Simplo*	*Duplo*	*Limit of Detection*	*Method*
1	*L-Alanine*	*mg/kg*	*23039.47*	*23067.14*	-	*11-6-4/MU (UPLC-PDA)*
2	*L-Arginine*	*mg/kg*	*44074.09*	*44202.56*	-	*11-6-4/MU (UPLC-PDA)*
3	*L-Aspartic Acid*	*mg/kg*	*38542.93*	*38577.13*	-	*11-6-4/MU (UPLC-PDA)*
4	*Glycine*	*mg/kg*	*63958.25*	*64064.73*	-	*11-6-4/MU (UPLC-PDA)*
5	*L-Glutamic Acid*	*mg/kg*	*51769.65*	*51821.35*	-	*11-6-4/MU (UPLC-PDA)*
6	*L-Histidine*	*mg/kg*	*2928.32*	*2960.36*	-	*11-6-4/MU (UPLC-PDA)*
7	*L-Isoleucine*	*mg/kg*	*24644.35*	*24660.02*	-	*11-6-4/MU (UPLC-PDA)*
8	*L-Cystine*	*mg/kg*	*153064.90*	*156926.33*	-	*11-7-2/MU (LC-MS/MS)*
9	*L-Leucine*	*mg/kg*	*59111.43*	*59198.60*	-	*11-6-4/MU (UPLC-PDA)*
10	*L-Lysine*	*mg/kg*	*21752.76*	*21773.54*	-	*11-6-4/MU (UPLC-PDA)*
11	*L-Methionine*	*mg/kg*	*101.95*	*103.29*	-	*11-7-2/MU (LC-MS/MS)*
12	*L-Tryptophan*	*mg/kg*	*3233.47*	*3314.47*	-	*11-6-5/MU (HPLC-PDA)*
13	*L-Valine*	*mg/kg*	*39614.90*	*39657.47*	-	*11-6-4/MU (UPLC-PDA)*
14	*L-Phenylalanine*	*mg/kg*	*33887.65*	*33825.97*	-	*11-6-4/MU (UPLC-PDA)*
15	*L-Proline*	*mg/kg*	*77631.16*	*77717.42*	-	*11-6-4/MU (UPLC-PDA)*
16	*L-Serin*	*mg/kg*	*52801.64*	*52887.59*	-	*11-6-4/MU (UPLC-PDA)*
17	*L-Threonine*	*mg/kg*	*15346.71*	*15375.82*	-	*11-6-4/MU (UPLC-PDA)*
18	*L-Tyrosine*	*mg/kg*	*18853.06*	*18891.57*	-	*11-6-4/MU (UPLC-PDA)*

Other amino acids, such as L-Glutamic Acid (51,769.65 – 51,821.35 mg/kg) and Glycine (63,958.25 – 64,064.73 mg/kg), contribute significantly to the structural and functional properties of proteins. L-glutamic acid, for example, is often associated with the umami taste of food products, while Glycine acts as a building block for collagen and other structural proteins. Branched-chain amino acids (BCAAs), including L-Leucine (59,111.43 – 59,198.60 mg/kg), L-Isoleucine (24,644.35 – 24,660.02 mg/kg), and L-Valine (39,614.90 – 39,657.47 mg/kg), were also found in significant amounts. BCAAs are known for their roles in energy metabolism, muscle recovery, and protein synthesis.

Overall, the analysis showed that the keratin samples were rich in amino acid content and variety; thus, they have the potential to contribute high nutritional value, especially for protein synthesis, tissue regeneration, and other metabolic functions.

3.8. LC-MS

The LC-MS analysis of keratin samples, as shown in Table 4, identified several compounds. It revealed the presence and abundance of several compounds with various molecular compositions. Chromatographic separation showed an interesting pattern where two compounds co-eluted at the earliest retention time, namely 0.962 min, specifically $C_9H_{11}NO_2$ (m/z 166.08582) and C_8H_9N (m/z 120.08082), with C_8H_9N (m/z 120.08082), with the abundance of C_8H_9N being much higher than $C_9H_{11}NO_2$. This co-elution indicated that both have similar physicochemical properties under certain chromatographic conditions. Furthermore, a compound with the molecular formula $C_8H_{12}N_6O$ (m/z 209.11652) was detected at a retention time of 1.187 minutes, showing a substantial abundance of 58735.33. While, the final compound, $C_3H_9N_2O_2$ (m/z 105.06462), was observed at a retention time of 4.212 minutes with the lowest abundance, i.e. 17749.24.

Table 4. LC-MS of keratin analysis

RT (Retention Time)	Mass m/z	Molecular Formula	Abundance
0.962	166.08582	$C_9H_{11}NO_2$	39833.04
0.962	120.08082	C_8H_9N	95239.18
1.187	209.11652	$C_8H_{12}N_6O$	58735.33
4.212	105.06462	$C_3H_9N_2O_2$	17749.24

Nitrogen and oxygen atoms in this molecular formula suggest a potential biological origin although the determination of the exact structure requires an additional analytical validation. This additional validation should include a comparison with native standards, MS/MS fragmentation pattern analysis, and complementary analytical techniques, such as NMR or IR spectroscopy. The significant variation in retention time, 0.962 - 4.212 minutes, showed fundamental differences in the interaction of these four compounds with the chromatography system. Of note, the co-elution observed at 0.962 min may benefit from the optimization of the method to produce a more selective separation.

Abundance patterns provide valuable information about sample composition, with C_8H_9N emerging as the dominant signal. However, it is essential to note that MS abundance may reflect actual concentration differences and varying ionization efficiencies at the specific MS conditions used [50]. This method requires internal standardization and validation using authentic references for more accurate quantitative analysis. The overall analytical approach can be improved by applying additional confirmation strategies, including MS/MS analysis for the structural elucidation and optimization of methods for separating co-eluting peaks, ultimately providing more accurate compound identification and quantitative analysis results.

3.9. NMR

^{1}H-NMR analysis was used to characterize keratin structure and identify any possible differences between α-helix and β-sheet in this protein. In this study, the ^{1}H-NMR spectrum of the keratin samples obtained showed various peaks related to the molecular structure of keratin, as shown in Fig. 9. The peak observed at 3.3 - 3.5 ppm indicated the presence of protons around groups that bond to electronegative atoms such as oxygen or nitrogen, possibly originating from hydroxyl (-OH) or amide groups in the keratin peptide chain. Signals at 2.4 - 2.5 ppm are often attributed to methylene groups (-CH_2-) adjacent to carbonyls (-C=O) or sulfur groups (-S-), which are the part of the cysteine residues in the keratin structure. In addition, the presence of a signal at 1.1 - 1.2 ppm indicates the presence of a methyl group (-CH_3) in the aliphatic environment, which can come from amino acid residues such as alanine and valine. Meanwhile, the peak at 0.7 - 0.9 ppm is related to the terminal methyl group frequently found in long aliphatic chains, indicating the presence of hydrophobic interactions in the protein structure [51].

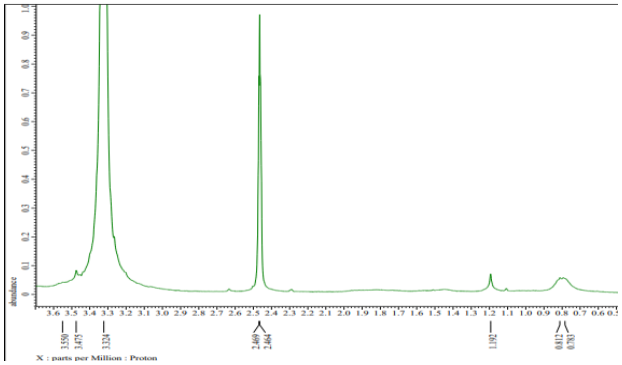

Fig. 9. The ^{1}H NMR spectrum (500 MHz) of keratin

This ^{1}H-NMR spectrum shows that the main structure of keratin is maintained during and after the extraction process. These emerging and observed peaks indicated that the hydrogen environment in keratin still maintains its typical structure, including carbonyl and amide groups, which play a role in the stability of this protein. However, the large number of peaks in this spectrum can also indicate variations in the chemical environment due to intra- and intermolecular

interactions, as mentioned in the research of Pourjavaheri et al. (2019), reporting that the keratin structure that appears often shows spectral complexity due to aggregation or structural changes occurred during the extraction process [37].

These ^{1}H-NMR spectrum results also indicated that intra- and intermolecular interactions in keratin remained after extraction, supporting its potential use as a biomaterial in tissue engineering and wound healing. The pore morphology observed from SEM characterization further supported this, indicating that keratin materials can have physical properties that support cell growth and nutrient exchange in biomedical applications.

Based on the results of ^{1}H-NMR analysis, it can be concluded that the extracted keratin still maintains its characteristic structure with various functional groups identified in the NMR spectrum. Although the solution NMR method is limited in distinguishing α-helix and β-sheet structures, the results indicated that intra- and intermolecular interactions in keratin were maintained after extraction. SEM characterization also supports that keratin has a morphology suitable for tissue engineering and wound healing applications. The results of FTIR analysis are also in line with ^{1}H-NMR analysis, showing that keratin maintains its characteristic functional groups, including amide, carbonyl, and peptide although there are changes in peak intensity due to pH variations. The peaks detected in FTIR, such as N-H and O-H stretching vibrations at 3250–3300 cm^{-1} and carbonyl C=O at 1700-1500 cm^{-1}, corresponded to the chemical shifts detected in NMR analysis. Changes in FTIR absorption patterns align with the results of NMR analysis, especially concerning intra- and intermolecular interactions in keratin. This fact indicates the stability of the keratin structure during the IL-UAE process.

3.10 Molecular Docking

Table 5. Docking result, binding energy, and cavity

Ligand	Binding Energy	Cavity Size
Cysteine	-4.2	1755
Leucine	-5	5105
Serine	-4.4	5105
Proline	-4.6	1755

Based on the results of our amino acid profiling, which showed the significant concentrations of various amino acids in duck feather keratin (Table 3), we then selected four representative amino acids (proline, cysteine, leucine, and serine) for our in silico study. A molecular docking study of protein kinase D (PKD) protein, as summarized in Table 5, showed the potential of these four amino acids as procollagen N-endopeptidase inhibitors. The analysis revealed that leucine had the highest binding affinity with a binding energy of -5.0 kcal/mol and a cavity size of 5105, followed by proline (-4.6 kcal/mol), serine (-4.4 kcal/mol), and cysteine (-4.2 kcal/mol). This negative binding energy value indicates the formation of a stable protein-ligand complex, where the more negative the value, the stronger the interaction. The large cavity size at the Leucine (5105) binding site also indicates an adequate space for an optimal bond formation, as shown in Fig. 10.

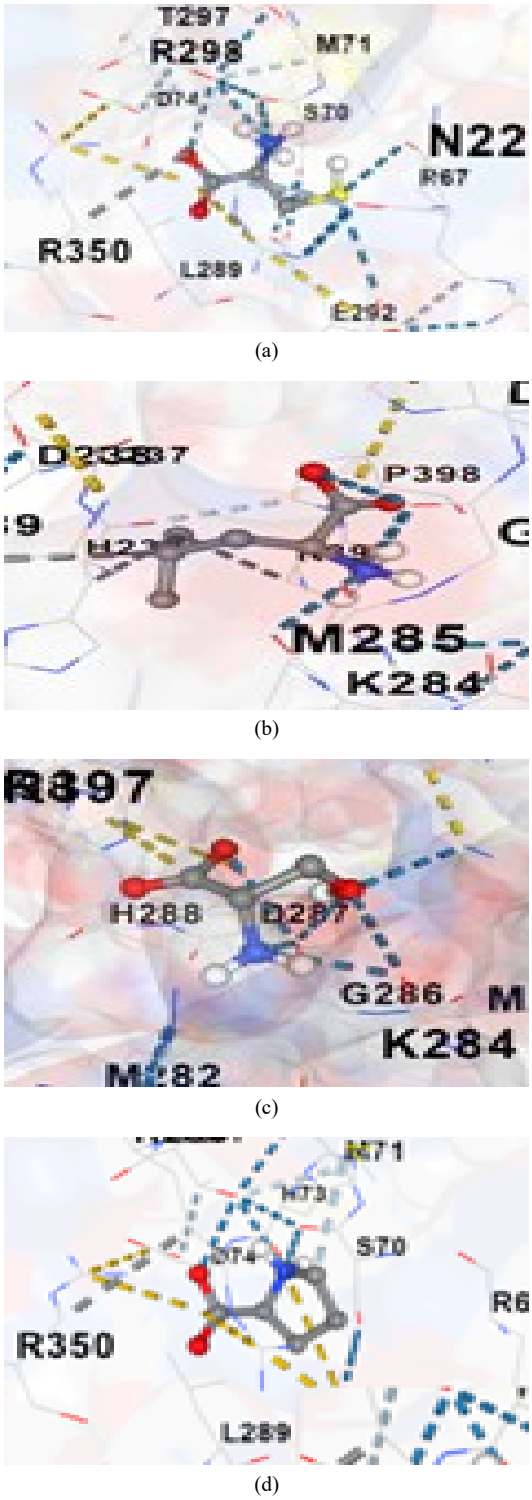

(a)

(b)

(c)

(d)

Fig. 10. Protein-ligand docking visualization of keratin-derived amino acids with procollagen N-endopeptidase: (a) cysteine showing binding interactions at a small cavity site; (b) leucine demonstrating strongest binding with optimal positioning in the large cavity; (c) serine displaying hydrogen bond formation with active site residues; and (d) proline exhibiting favorable conformation at the binding interface

Procollagen N-endopeptidase (also known as ADAMTS-2) plays a critical role in the processing of procollagen to mature

collagen by cleaving the N-terminal propeptide of type I, II, and III procollagens. The inhibition of this enzyme is particularly significant in relation to protein kinase D (PKD), a serine or threonine protein kinase involved in diverse cellular processes including cell proliferation, protein transport, and extracellular matrix remodeling. The interplay between PKD signaling and collagen processing via procollagen N-endopeptidase represents an important regulatory mechanism in tissue homeostasis [54].

Previous studies have demonstrated that PKD activation can upregulate procollagen N-endopeptidase activity, leading to enhanced collagen maturation and deposition. This process is particularly relevant in conditions characterized by excessive fibrosis and abnormal extracellular matrix remodeling. By inhibiting procollagen N-endopeptidase, the collagen processing pathway can be modulated, potentially attenuating PKD-mediated fibrotic responses. Additionally, the inhibition of this enzyme may influence PKD-dependent cellular signaling cascades, offering a novel approach to regulate PKD activity and its downstream effects on tissue remodeling and cell behavior [55,56].

As the inhibitors of procollagen N-endopeptidase, these four amino acids could inhibit procollagen processing into mature collagen, affecting extracellular matrix formation and cyst development in PKD patients. With its lowest binding energy, Leucine showed the most significant potential as a lead compound for developing more effective inhibitors. Protein visualization showed a uniform distribution of binding sites with consistent center coordinates and size parameters among all experiments, confirming the reliability of the docking results. These findings have opened new avenues in developing procollagen N-endopeptidase inhibition-based PKD therapeutics with leucine as the lead candidate for further optimization. These computational findings complement the experimental results on keratin extraction and characterization, providing a molecular-level understanding of how duck feather keratin might interact with key proteins involved in bone metabolism. The in silico approach allows us to predict potential biological interactions before proceeding to more resource-intensive in vitro and in vivo studies, thus guiding the rational design of keratin-based biomaterials for specific biomedical applications.

4. Conclusion

This study successfully optimized the extraction of keratin from duck feathers using the Ionic Liquid-assisted Ultrasonic-Assisted Extraction (IL-UAE) method with pH parameters showing a significant effect on the extraction results. The highest yield of 82% was obtained at pH 3, while the lowest yield of 33% occurred at pH 6. The extraction conditions at pH 3 were proven to support the formation of stable and uniform keratin coacervates, essential for biomaterial applications. Functional group analysis using FTIR showed that a β-sheet structure dominated the resulting keratin. Meanwhile, testing with SDS-PAGE showed the presence of the main keratin band with a molecular mass of 10-15 kDa. Morphologically, SEM observations showed a uniform structure without additional cross-linking during the fabrication process. Thermal analysis revealed that thermal degradation of keratin occurred in three stages, with a total mass reduction reaching 73.5% at a temperature of 700°C. In addition, amino acid profiling showed L-cysteine content as the main component, which plays an important role in tissue regeneration. LC-MS data provide in-depth information about the composition of keratin compounds, including various functional groups such as hydrocarbon chains, carbonyl, hydroxyl, and amino groups. In addition to the successful extraction of high-quality keratin from duck feathers, through molecular docking studies, the results of this study also showed the potential of keratin as an inhibitor of procollagen N-endopeptidase, which has an important role in the biomedical field, especially in tissue regeneration. On the other hand, utilizing livestock waste in high-value resources in this study is expected to support a circular economy by reducing the negative impact of organic waste on the environment and sustainable material innovation.

Acknowledgments

The authors would like to thank the Ministry of Education, Culture, Research, and Technology of the Republic of Indonesia for their financial support. Author Contributions: M.M.S.B: writing, review, and editing; N.K.: conceptualization, methodology, formal analysis, original manuscript writing, review, and validation; M.T.A.: manuscript review and editing, data analysis and curation; S.A.D.: writing review and editing, project administration, and validation; A.N.A.H.: writing, writing validation; A.K.: writing, investigation, resources, and review; M.A.N.: writing review, editing; F.S.: writing review, editing; L.I.: writing review, editing; K.R.: writing review, editing, and project administration. All authors have read and approved the published version of the manuscript.

Funding: This research was funded by the Ministry of Education, Culture, Research and Technology of the Republic of Indonesia.

Conflict of Interest: The authors declared no conflict of interest.

References

1. C. Sing, T. Lin, S. Bartholomew, J.S. Bell, C. Bennett, K. Beyene, et al., *Global Epidemiology of Hip Fractures: Secular Trends in Incidence Rate, Post-Fracture Treatment, and All-Cause Mortality*, J. Bone Miner. Res. 38(8) (2023) 1064-1075.
2. Y. Rong, X. Liang, K. Jiang, H. Jia, H. Li, B. Lu, et al., *Global Trendsin Research of Programmed Cell Deathin Osteoporosis: A bibliometric and Visualized Analysis (2000–2023)*, Orthop. Surg. 16 (2024) 1783-1800.
3. M.A. Clynes, N.C. Harvey, E.M. Curtis, N.R. Fuggle, E.M. Dennison, C. Cooper, *The epidemiology of osteoporosis*, Br. Med. Bull. 133(1) (2020) 105-117.
4. M.A. Clynes, L.D. Westbury, E.M. Dennison, J.A. Kanis, MK. Javaid, N.C. Harvey, et al., *Bone densitometry worldwide: a global survey by the ISCD and IOF*, Osteoporos. Int. 31 (2020) 1779-1786.
5. M. Zhang, R. Lin, X. Wang, J. Xue, C. Deng, C. Feng, et al., *3D printing of Haversian bone–mimicking scaffolds for multicellular delivery in bone regeneration*, Sci. Adv. 6(12) (2020) eaaz6725.
6. H. Shanshan, K. Nie, J. Li, Q. Sun, X. Wang, X. Li, et al., *3D Electrospun Nanofiber-Based Scaffolds: From Preparation and Properties to Tissue Regeneration Applications*, Stem Cells Int. 22 (2021) 8790143.
7. A.R. Khan, N. S. Grewal, Z. Jun, F.M.O. Tawfiq, F. Tchier, R.M. Zulqarnain, et al., *Raising the Bar: Progress in 3D-Printed Hybrid Bone Scaffolds for Clinical Applications: A Review*, Sage J. 33 (2024) 1-17.

8. M. Krishani, W.Y. Shin, H. Suhaimi, N.S. Sambudi, *Development of Scaffolds from Bio-Based Natural Materials for Tissue Regeneration Applications: A Review*, Gels 9 (2022) 100.
9. Y. Kim, S. Vijayavenkataraman, G. Cidonio, *Biomaterials and scaffolds for tissue engineering and regenerative medicine*, BMC Methods 1(2) (2024).
10. M.S.B. Reddy, D. Ponnamma, R. Choudhary, K.K. Sadasivuni, *A Comparative Review of Natural and Synthetic Biopolymer Composite Scaffolds*, Polymers 13 (2021) 1105.
11. A.E. Eldeeb, S. Salah, N.A. Elkasabgy, *Biomaterials for Tissue Engineering Applications and Current Updates in the Field: A Comprehensive Review*, AAPS PharmSciTech. 23 (2022) 267.
12. L.E. Rojas-Martíneza, C.G. Flores-Hernandeza, L.M. López-Marínb, A.L. Martinez-Hernandeza, S.B. Thoratc, C.D. Reyes Vasquez, et al., *3D printing of PLA composites scaffolds reinforced with keratin and chitosan: Effect of geometry and structure,* Eur. Polym. J. 141 (2020) 110088.
13. H. Zhang, F. Su, X. Ma, G. Zhao, *Brief introduction of keratin and its biological application, especially in drug delivery,* Emerg. Mater. 4 (2021) 1225-1242.
14. J.E. Plowman, R.E. Miller, A. Thomas, A.J. Grosvenoer, D.P. Harland, S. Deb-Choudhury, *Adetailed mapping of the readily accessible disulphide bonds in the cortex of wool fibres*, Proteins 89 (2021) 708-720.
15. M. Konop, A.K. Laskowska, M. Rybka, E. Klodzinska, D. Sulejczak, R.A. Schwartz, *Keratin Scaffolds Containing Casomorphin Stimulate Macrophage Infiltration and Accelerate Full-Thickness Cutaneous Wound Healing in Diabetic Mice*, Molecules 26 (2021) 2554.
16. A.J. Morwood, I.A. El-Karim, S.A. Clarke, F.T. Lundy, *The Role of Extracellular Matrix (ECM) Adhesion Motifs in Functionalised Hydrogels,* Molecules 28 (2023) 4616.
17. S. Banasaz, V. Ferraro, *Keratin from Animal By-Products: Structure, Characterization, Extraction and Application—A Review*, Polymers 16 (2024) 1999.
18. O.A. Meko, S.O. Eraga, M.I. Arhewoh, *Effect of extraction parameters on some properties of keratin obtained from waste chicken feathers*, Trop. J. Nat. Prod. Res. 8(6) (2024) 7423-7430.
19. S.D. Marliyana, T.I.S.T. Dewi, T. Kusumaningsih, *Extraction of β-keratin from poultry feather waste using sodium metabisulfite and sodium dodecyl sulfate*, Malays. J. Anal. Sci. 28(1) (2024) 116-126.
20. S. Banasaz, V. Ferraro, *Keratin from animal by-products: structure, characterization, extraction and application—A review*, Polymers 16(14) (2024) 1999.
21. M. Skerget, M. Colnik, L.F. Zemljic, L. Gradisnik, T.Z. Semren, B.T. Lovakovic, et al., *Efficient and green isolation of keratin from poultry feathers by subcritical water*, Polymers 15(12) (2023) 2658.
22. S.G. Giteru, D.H. Ramsey, Y. Hou, L. Cong, A. Mohan, A.E-D.A. Bekhit, *Wool keratin as a novel alternative protein: A comprehensive review of extraction, purification, nutrition, safety, and food applications*, Compr. Rev. Food Sci. Food Saf. 22(1) (2022) 643-87.
23. Y.S. Khoo, T.C. Tjong, J.W. Chew, X. Hu, *Techniques for recovery and recycling of ionic liquids: A review*, Sci Total Environ. 922 (2024) 171238.
24. R. Salas, R. Villa, F. Velasco, F.G. Cirujano, S. Nieto, N. Martin, et al., *Ionic liquids in polymer technology*, Green Chem. 27 (2025) 1620.
25. C.L.B. Reis, A.V.F. Carvalho, T.B.A.R. Miguel, E.C. Miguel, D.S. Zampieri, M.V.P. Rocha, et al., *Green synthesis of choline-based ionic liquids and utilization in the extraction of biomolecules from Limnospira platensis microalgae*, J. Appl. Phycol. 16(1) (2024) 151.
26. X. Lin, K. Jiang, X. Liu, D. Han, *Review on development of ionic liquids in lignocellulosic biomass refining*, J. Mol. Liq. 359(24) (2022) 119326.
27. F. Yang, C. Chen, D. Ni, Y. Yang, J. Tian, Y. Li, et al., *Effects of fermentation on bioactivity and the composition of polyphenols contained in polyphenol-rich foods: A review*, Foods 12(17) (2023) 3315.
28. N. Nayak, R.R. Bhujle, N.A. Nanje-Gowda, S. Chakraborty, K. Siliveru, J. Subbiah, et al., *Advances in the novel and green-assisted techniques for extraction of bioactive compounds from millets: A comprehensive review*, Heliyon 10 (2024) e30921.
29. M. Kammoun, A. Margellou, V.B. Toteva, A. Aladjadjiyan, A.F. Sousa, S.V. Luis, et al., *The key role of pretreatment for the one-step and multi-step conversions of European lignocellulosic materials into furan compounds*, RSC Adv. 13 (2023) 21587-21612.
30. R.S. Abolore, S. Jaiswal, A.K. Jaiswal, *Green and sustainable pretreatment methods for cellulose extraction from lignocellulosic biomass and its applications: A review*, Carbohydr. Polym. Technol. Appl. 7 (2024) 100396.
31. D. Kim, S-G. Kang, Y.K. Chang, M. Kwak, *Two-step macromolecule separation process with acid pretreatment and high-shear-assisted extraction for microalgae-based biorefinery*, Sustainability 16(17) (2024) 7589.
32. P. Bharmoria, A.A. Tietze, D. Mondal, T.S. Kang, A. Kumar, M.G. Freire, *Do ionic liquids exhibit the required characteristics to dissolve, extract, stabilize, and purify proteins? Past-present-future assessment*, Chem Rev. 124(6) (2024) 3037-3084.
33. S.K. Panja, S. Kumar, B. Haddad, A.R. Patel, D. Villemin, H-M Amine, et al., *Role of multiple intermolecular H-bonding interactions in molecular cluster of hydroxyl-functionalized imidazolium ionic liquid: an experimental, topological, and molecular dynamics study*, Physchem. 4(4) (2024) 369-388.
34. C. Polesca, A.A. Gatta, H. Passos, J.A.P. Coutinho, J.P. Hallett, M.G. Freire, *Sustainable keratin recovery process using a bio-based ionic liquid aqueous solution and its techno-economic assessment*, Green Chem. 25 (2023) 3995-4003.
35. A. Cordova, S. Catalan, V. Carrasco, F.O. Farias, J. Trentin, J. Lopez, et al., *Sustainable assessment of ultrasound-assisted extraction of anthocyanins with bio-based solvents for upgrading grape pomace Cabernet Sauvignon derived from a winemaking process*, Ultrason. Sonochem. 112 (2025) 107201.
36. S. Kong, Y. Liu, R. Tang, Q. Liao, D. Bai, D. Lv, et al., *Ultrasound-assisted extraction of prenylated flavonoids from Sophora flavescens: Optimization, mechanistic characterization, antioxidant and anti-inflammatory activities*, Ind. Crops Prod. 225 (2025) 120559.
37. F. Pourjavaheri, S.O. Pour, O.A.H. Jones, P.M. Smooker, R. Brkljača, F. Sherkat, et al., *Extraction of keratin from waste chicken feathers using sodium sulfide and l-cysteine*, Process Biochem. 82 (2019) 205-214.
38. L. Machado-Carvalho, T. Martins, A. Aires, G. Marques, *Optimization of Phenolic Compounds Extraction and Antioxidant Activity from Inonotus hispidus Using Ultrasound-Assisted ExtractionTechnology*, Metabolites 13(4) (2023) 524.
39. D. Rosarina, R.N. Dimas, N.S.R. Chandra, E.F. Sari, H. Hermansyah, *Optimization of Ultrasonic-Assisted Extraction (UAE) Method Using Natural Deep Eutectic Solvent (NADES) to Increase Curcuminoid Yield from Curcuma longa L., Curcuma xanthorrhiza, and Curcuma mangga Val.*, Molecules 27(18) (2022) 6080.
40. J. Sun, G.M. Santiago, F. Yan, W. Zhou, P. Rudolf, G. Portale, et al., *Bioinspired Processing of Keratin into Upcycled Fibers through pH-Induced Coacervation*, ACS Sustain. Chem. Eng. 11(5) (2023) 1985-1994.
41. A. Mengistu, G. Andualem, M. Abewaa, D. Birhane, *Keratin extraction optimization from poultry feather using response surface- Box-Behnken experimental design method*, Results Eng. 22 (2024) 102360.
42. S. Perez-Vila, M. Fenelon, D. Hennessy, J.A. O'Mahony, L.G. Gomez-Mascaraque, *Impact of the extraction method on the composition and solubility of leaf protein concentrates from perennial ryegrass (Lolium perenne L.)*, Food Hydrocoll. 147(A) (2024) 109372.
43. K. Gulza, R.B. Arfi, K. Mougin, C. Vaulot, L. Michellin, L. Josien, et al., *Development of novel and ecological keratin/cellulose-based composites for absorption of oils and organic solvents*, Environ. Sci. Pollut. Res. 28 (2021) 46655–46668.
44. R.A. Pérez, B.Albero, *Ultrasound-assisted extraction methods for the determination of organic contaminants in solid and liquid samples*, Trends Anal. Chem. 166 (2023) 117204.
45. A.B.D. Nandiyanto, R. Oktiani, R. Ragadhita, *How to Read and Interpret FTIR Spectroscope of Organic Material*, Indones. J. Sci. Technol. 4(1) (2019) 97-118.
46. M. Škerget, M. Colnik, L.F. Zemljic, L. Gradinik, T.Z. Semren, B.T. Lovakovic, et al., *Efficient and Green Isolation of Keratin from Poultry Feathers by Subcritical Water*, Polymers 15(12) (2023) 2658-2658.
47. S. Alvarez, *Development of innovative bio-based films with keratin extracted from duck feathers*, Pau, France: Universite de Pau et des Pays de l'Adour, 2024.
48. J. Qiu, C. Wilkens, K. Barrett, A.S. Meyer, *Microbial enzymes catalyzing keratin degradation: Classification, structure, function*, Biotechnol. Adv. 44 (2020) 107607.
49. Y. Su, E.P. Hessou, E. Colobo, G. Belletti, A. Moussadik, I.T. Lucas, et al., *Crystalline structures of l-cysteine and l-cystine: a combined theoretical and experimental characterization*, Amino Acids 54(8) (2022) 1123-1133.
50. A. Henderson, L.M. Heaney, S. Rankin-Turner, *Advancements in Ambient Ionisation Mass Spectrometry in2024: An Annual Review*, Anal. Sci. Adv. 6 (2025) e7000.
51. R. Gunawan, A.B.D. Nandiyanto, *How to Read and Interpret 1H-NMR and 13C-NMR Spectrums*, Indones. J. Sci. Technol. 6(2) (2021) 267-298.
52. R. Wang, H. Tong, *Preparation Methods and Functional Characteristics of Regenerated Keratin-Based Biofilms*, Polymers 14(21) (2022) 4723.
53. N. Senthilkumar, S. Chowdhury, P. Sanpui, *Extraction of keratin from keratinous wastes: current status and future directions*, J. Mater. Cycles

Waste Manag. 25 (2023) 1–16.
54. K. Zuniga, N. Ghousifam, J. Sansalone, K. Senecal, M.V. Dyke, M.N. Rylander, *Keratin Promotes Differentiation of Keratinocytes Seeded on Collagen/Keratin Hydrogels*, Bioengineering 9(10) (2022) 559.
55. Q. Chen, Y. Pei, M.G. Abu-Kaya, *Structure, extraction, processing, and applications of collagen as an ideal component for biomaterials - a review*, Collagen Leather 5(20) (2023).
56. M. Rajabi, A. Ali, M. McConnell, J. Cabral, *Keratinous materials: Structures and functions in biomedical applications*, Mater. Sci. Eng. C. 110 (2020) 110612.